Aspects of the Local Circulation at the Grand Canyon during the Fall Season

L. P. STEARNS

NOAA/Environmental Research Laboratory, Air Resources Laboratory, Geophysical Monitoring for Climatic Change, Boulder, CO 80303

(Manuscript received 6 September 1986, in final form 13 April 1987)

ABSTRACT

The atmosphere and circulation of air within, above, and around the Grand Canyon of the Colorado River was studied from an instrumented aircraft and from ground-based instruments in September and October 1984. Several patterns were identified. The nighttime formation of stabilized layers and infrared cooling did not necessarily guarantee a downslope and a downstream flow. Morning observations showed early formation of thermal patterns, which increased during the day until, under clear skies, turbulent mixing would disrupt the stable layers above the canyon in September. October solar heating seemed insufficient to totally disrupt the stable layers above the canyon, and only limited areal segments displayed instability at the rim level. The depth of the turbulent mixing is a function of sky cover and cloud thickness. The amount of influence of the large-scale air motion depends on the orientation of the canyon relative to the direction of this motion.

1. Introduction

Air circulation within the boundaries of a canyon is influenced by many factors within the canyon, as well as the synoptic conditions surrounding the canyon. Among these local conditions are the width and depth of the canyon; its geographical orientation, which influences its thermal patterns; the location and formation of the buttes and other irregular features, which not only affect the thermal patterns but create secondary and tertiary wind flows; and the types of soils, soil moisture, and shrubbery within the canyon. Therefore, in describing the atmosphere of a canyon, the uniqueness of the canyon must be included.

Numerous studies have been made, but mostly about mountain valley circulation characteristics. Banta and Cotton (1981) found two wind regimes on a dry day in a broad mountain valley: a downslope drainage wind at night due to cooling of the slope surfaces, and upslope winds in the day due to solar heating. They also found good mixing within the convective boundary layer. The Atmospheric Studies in Complex Terrain (ASCOT) program produced a volume of information, especially on nocturnal drainage flows in deep valleys. Complex slopes, valleys, and basin effects are thoroughly discussed in Dickerson and Gudiksen (1983). Particular interest is drawn to the counterflow above the drainage flow (Post and Neff, 1986) and the Doppler scans of not only the nocturnal flow but also the thermally driven up-valley winds.

Destruction of temperature inversions 3.5 to 5.0 h after sunrise was investigated by Bader and Mc Kee (1985) and in earlier work by Whiteman (1982), both for a deep mountain valley, but the applicability of their conclusions has not been tested within a canyon.

Research for this paper was conducted in the fall of 1984 in a portion of the Grand Canyon of the Colorado River in Arizona. This canyon is 446 km long and averages 16 km in width. The North Rim varies from 2.3 to 3.9 km MSL in altitude, while the South Rim varies from 1.8 to 2.2 km MSL. The average depth is 1.7 km measured from the North Rim. The interior of the canyon contains many buttes and plateaus. The walls are sometimes vertical, especially near the rims and sometimes slope from 10° to 45° from the horizontal. The Grand Canyon possesses five of the seven life zones ascribed to the Northern Hemisphere and therefore presents a unique atmosphere compared with other less complex canyons.

Knowledge of the behavior of the areal and the internal wind patterns of the canyon has a variety of applications: 1) The canyon attracts numerous visitors each year, but according to visibility observations this visual resource has been diminished because of trapped pollution; 2) The National Park Service, in order to maintain the natural state of the wooded areas on both the North and South Rims must burn the understory on these rims. The wind directions of the local circulation must be understood so that smoke does not descend into the canyon and become trapped during the burn times, which sometimes extend to four days; 3) Air tours by helicopters and small aircraft, which descend into the canyon, are made daily; therefore, knowledge of vertical air currents, which have been measured up to 50 m s^{-1} in the afternoon where thermal currents are at a maximum (Sinclair, personal communication, 1986) can help promote air safety.

The features that are examined and discussed in this paper include possible diurnal variation in the wind flow within and abutting the canyon, the heating of the canyon walls, and comments about stability and buoyancy within the canyon.

2. Research area

A complete study of the entire Grand Canyon is a monumental task. The orientation of the canyon varies from north–south to east–west with all directions in-between. The portion of the canyon investigated for this study was the eastern end where visibility becomes most important for tourists. The area is pictured in Fig. 1. It extends, roughly, from Bright Angel Canyon in the west to the Painted Desert in the east. A few of the buttes such as Vishnu Temple and Wotans Throne are depicted in the figure, but not all. In this section of the canyon, the North Rim has an MSL altitude of 2438 m, increasing to the north to over 2600 m. The South Rim varies in the research area from 2072 m MSL near Comanche Point in the east to about 2285 m MSL farther west; the average MSL altitude for the South Rim is 2280 m. South of the rim, the area slopes downward and is broken by some shallow basins. The town of Tusayan is one such basin with an altitude of 2010 m MSL and the Grand Canyon Village, not shown in Fig. 1, with an altitude of 2091 m MSL is another. Grand Canyon Village is close to the South Rim but west of the figure boundary.

Surrounding this canyon area on both the north and south are the Grand Canyon National Park and the Kaibab National Forest. The two rims have only the

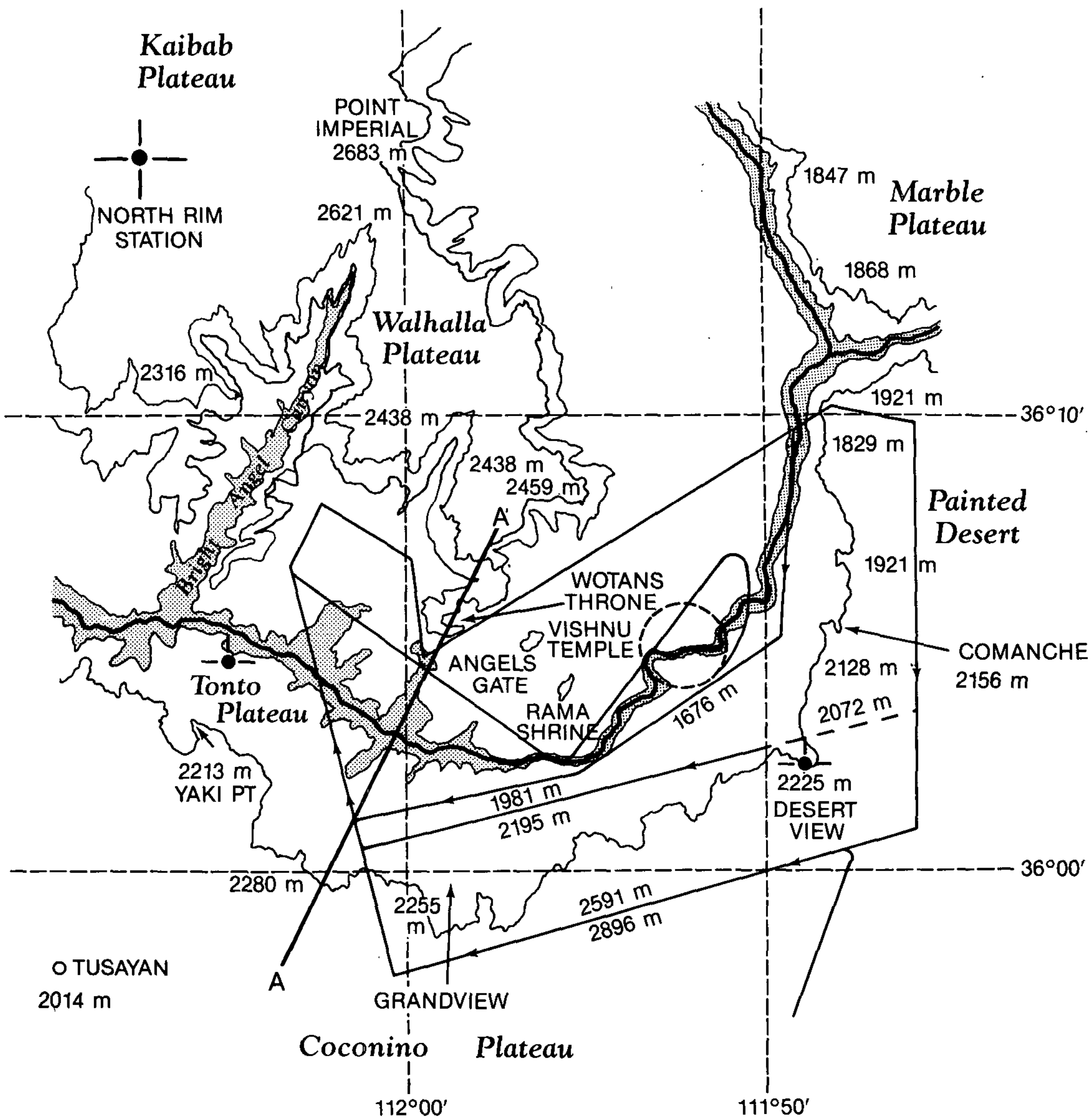

FIG. 1. Research area of the Grand Canyon showing flight paths (solid lines), profile area (dashed circle), and three permanent ground stations (stars). The cross section in Fig. 2 was taken along line A–A′.

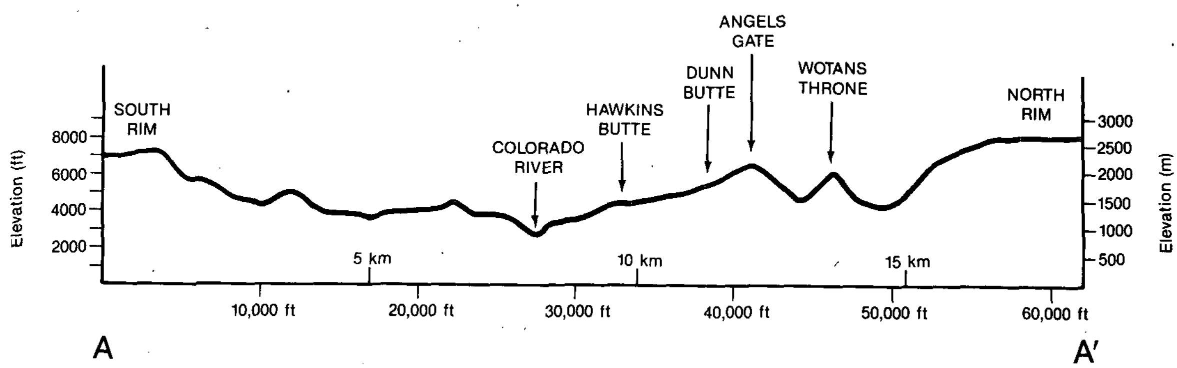

FIG. 2. Cross section A–A′ of Fig. 1.

name of the forest and park in common. The climatology of the two areas is different, as exemplified by the annual precipitation which is 600–750 mm (including melted snow) on the North Rim and only 230 mm on the South Rim.

Within the confines of the research area, the distance across the canyon ranges from 9.5 to 18.75 km. Many smaller canyons feed into the main basin, each of varying dimensions and consisting of other smaller canyons abutting them.

3. Aircraft instrumentation and flight path and ground equipment

An aircraft, a Cesna T207, was equipped with instruments to measure temperature, dewpoint, wind speed and direction, and infrared radiation. These included a Rosemount total air temperature sensor, a Cambridge dewpoint sensor, a Barnes radiometer operating in the 15 μm spectral passband, a gust probe, a downward-facing radiometer (for interface temperatures) and a sideward-facing radiometer (for wall temperatures) with 9.5–11.5 and 8.0–14.0 μm optical passbands, and the usual pitch, roll, pressure altitude, and airspeed equipment. The data were recorded on 9-track magnetic tape. Visual sightings and compass readings were used to position the aircraft.

The flight paths of the aircraft are superimposed on Fig. 1 and were repeated in each expedition to the depth that was safe for the aircraft for the individual penetrations. Using the patterns depicted in Figs. 1 and 3, the aircraft ascended to 2896 m over the South Rim (No. 3 in Fig. 3). It continued at this altitude through a pattern shown in Fig. 1 to the southern end of the east rim (No. 11 of Fig. 3) where it descended to 2591 m. The flight path at this altitude is identical to the

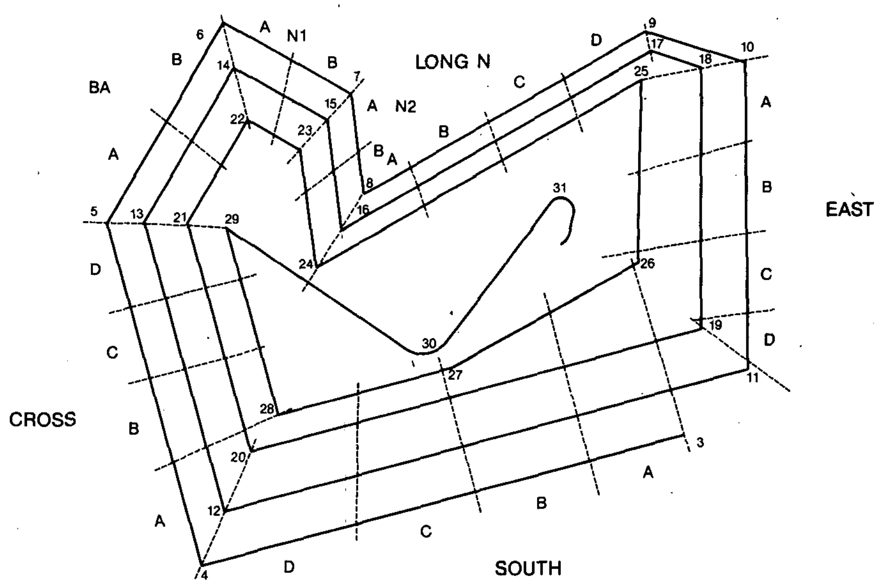

FIG. 3. Conceptual drawing of the flight paths, showing the segments used in data evaluation.

one at the higher altitude. At point 19 (Fig. 3), the aircraft descended to 2195 m to obtain wall data within the canyon. It made one full pattern identical to the previous ones, with the exception of the south and east rim, to point 26 (Fig. 3) where it descended to 1981 m and traversed the innermost flight path depicted in Fig. 1. The final descent, used only on September mornings, was at 1676 m and identical to that of 1981 m. At the conclusion of the flight patterns, an upward spiral profile was flown (dashed circle, Fig. 1) until an altitude of 2896 m was reached and then the aircraft returned to the airport which is west of Tusayan off the map. The patterns were chosen to be equal distances from the walls to ensure aircraft safety and minimize relative wall temperature corrections. Turbulence and sinking motions, especially in the afternoon, would occasionally force elimination of the penetration to even 1981 m.

Figure 3 illustrates the 19 segments into which the canyon was broken for research purposes. They are South A, B, C, D, CROSS B, C, D (A contains only two levels which are partly over the rim and partly over the canyon); BA A, B, N1 A, B, N2 A, B; LONG N A, B, C, D; EAST A, AND B (C and D have no lower layers). The purpose of these divisions was to obtain the integrated net areal measurements for research purposes.

Continuous measurements of temperature, moisture, and wind speed and direction at 10 m were made by HANDAR Equipment at sites on the North Rim, (North Rim Station) South Rim, (Desert View), and the Tonto Plateau in the canyon just north of Yaki Point. These permanent stations are marked by stars on Fig. 1. Unfortunately, only three wind stations were erected. This was partly due to budget restraints, and also partly due to the paucity of relatively flat and tree-free areas to obtain impartial data. Observations and measurements were continuous for 2 yr. Figure 2 represents a cross section of the canyon showing the irregularities of the features. The location of this cross section is depicted on Fig. 1 as A–A′.

4. Results

The synoptic surface chart of 29 September shows a 1032 mb high-pressure area located northeast of the canyon area centered in Colorado. The nearest low-pressure area is over the Baja Peninsula to the south which is not visible in any of the upper-air charts. Its pressure is 1012 mb. A very weak cold front associated with this low is east and south of the Grand Canyon. The canyon area is influenced by ridging both at the surface and aloft. All surrounding stations are reporting clear skies. On 29 October, the nearest high-pressure area is centered over Lake Michigan and there are no low-pressure areas over the United States. The upper-air flow is also uneventful showing no high or low-pressure areas in the United States. Lower pressure values are to the north. Surface weather shows no frontal systems near the canyon and no dramatic weather information. The morning charts show mostly clear stations surrounding the station except a few cirrus to the north. The afternoon surrounding stations show variable cloudiness. The pattern was repeated the next day.

There were 5 flights in September and 16 in October 1984, half in the morning, the other half about 1.5 h before sunset. Simultaneously, the three surface stations recorded data. Figures 4 and 5 show the wind roses that were plotted for night and day during the periods of investigation and are typical of the data obtained. The first notable feature is the wind directions measured on Tonto Plateau within the canyon. The nighttime September data suggest that a downstream (east-southeast) nocturnal drainage is occurring. During October nighttime the reverse is true. A large ellipse eccentricity with the major axis of the ellipse along the wind vector (as occurs at night) indicates a near-constant wind direction and more varying speed, while a smaller ellipse eccentricity (as occurs during the day) denotes more variable wind direction. From the location of this station, a downslope wind would be from the southwest.

In order for data from the station on the South Rim to reflect canyon influence, the wind direction would have to be from the northwest; if there is any outflow from the canyon at this location, especially in the latter part of the day, it is not evident from the wind roses or more close examination of the raw data. Conversely, a flow toward the canyon is not observed. Instead, the flow is more along the canyon rim.

The North Rim station located on the edge of a basin shows a very light drainage flow at night which is directed toward the canyon in September. The basin, which contains some hills, is very broad and has a depth of only 15–30 m. Therefore, it should easily be disrupted by synoptic flow.

However, throughout all the September–October research missions in the day, the North Rim station showed winds that varied from south-southwest to west-southwest with one exception at 1630 MST 28 September when the wind direction was from the west-northwest. This suggests that the local basin had an effect on the wind direction at this site, probably due to orientation and some thermal patterns. Referring to Table 1, it is interesting to note that during the September morning flight time, only the North Rim station records a near southwest flow, as opposed to the easterly component at all the other surface wind sites. This suggests that a basin upstream flow was occurring at that time. Also, note that where the winds had an easterly component (September) they were weaker than those with a westerly component.

We have selected three aircraft datasets, one from September and two from one day in October to present here for comparison and contrast. In each of these two days, 29 September and 29 October, the sky was clear

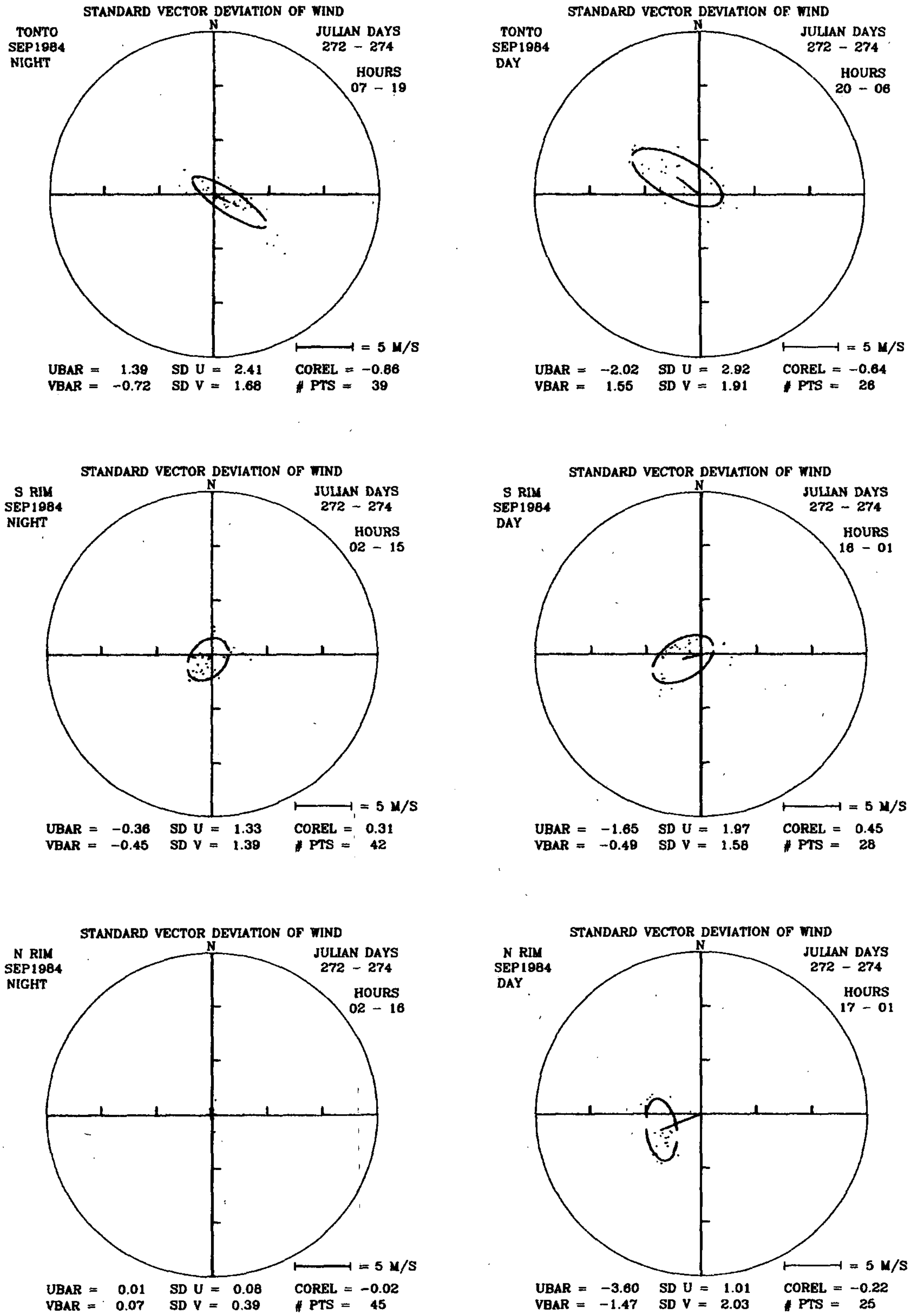

FIG. 4. Wind roses from September research period from each of the three permanent ground stations, night and day. Ellipses indicate one standard deviation of the wind averages. Time is UTC.

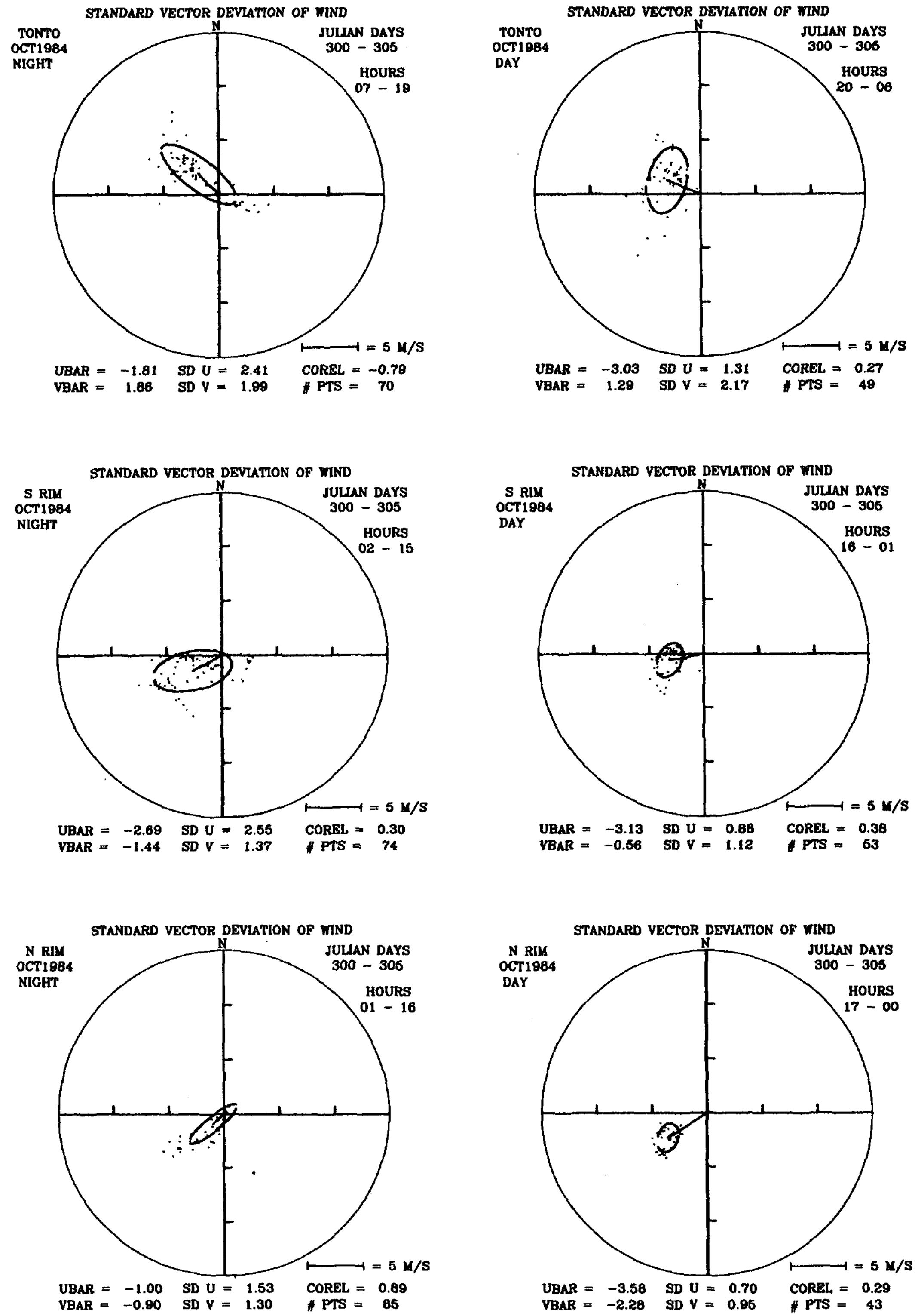

FIG. 5. As in Fig. 4 but for the October research period.

TABLE 1. Wind directions and speeds (m s^{-1}) for three selected data sets.

Date (1984)	Time (MST)	Synoptic flow Surface	700 mb	Tusayan airport	Tonto	South rim	North rim
29 Sept.	0928–1011	NE	NNW	ESE/2.6	SE/1.2	E/2.7	WSW/3.1
29 Oct.	0916–1039	S	S	S/7.7	WNW/4.5	W/3.6	WSW/2.7
29 Oct.	1552–1659	WSW	SW	WSW/6.2	WNW/2.7	W/3.6	WSW/4.0

in the morning and broken (0.6–0.9 sky cover) in the afternoon. The wind directions at each of the surface stations are listed in Table 1, along with the surface synoptic flow taken from streamlines from the 3-hourly surface synoptic charts and the airport data taken during the time of the aircraft data acquisition.

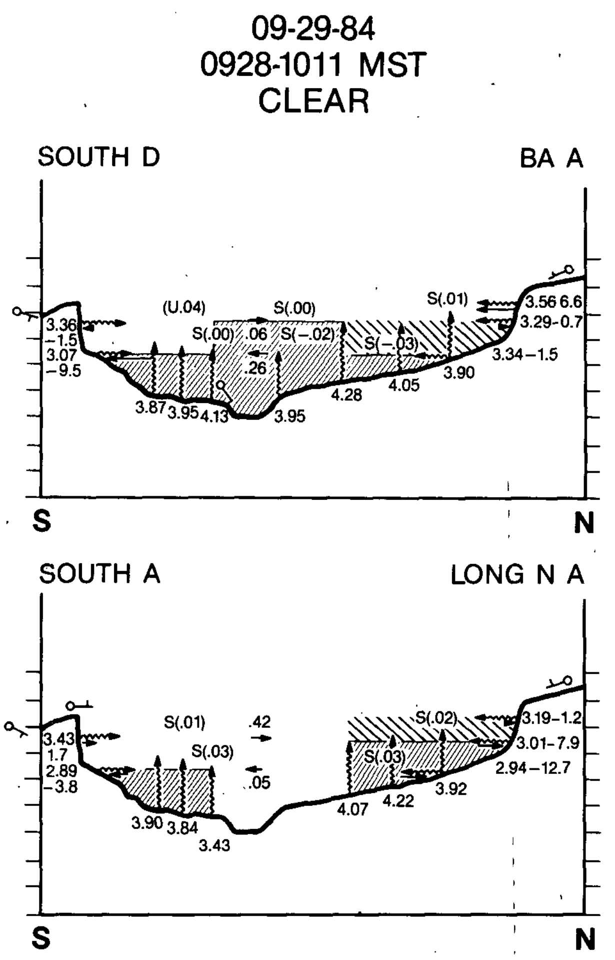

FIG. 6. Artist's conception of measured and calculated data from the 29 September 1984 morning flight. Radiation values (next to wavy-shafted arrows) are in J m^{-2} day^{-1} $\times 10^7$; temperature differentials (next to straight-shafted arrows along the walls) are in K; stability is indicated by S (stable) or U (unstable); acceleration values (in parentheses next to stability indicators) are in m s^{-2}. Arrows in the center of the canyon depict level radiation differentials and direction of flow. The wind barbs are for the ground stations at their approximate locations. Shading indicates infrared warming. Reverse hatch indicates neither warming or cooling. Sunrise was at 0620 MST (1320 UTC) and sunset at 1815 MST (0115 UTC). See Fig. 3 for identification of segments of the canyon.

The September aircraft missions were flown at a greater depth into the canyon than the October missions; therefore, more detail was obtained at lower levels, but less was learned about the stability above the canyon. Figure 6 shows an artist's concept of cross sections of the canyon in September, the parameters measured and calculated, and wind barbs of the ground station placed at the approximate locations. Stability is noted in the layer where it was monitored; the acceleration for the layer is also noted and is in parentheses. The corrected radiation emitted by the walls and floors is in J m^{-2} day^{-1} $\times 10^7$, and the difference between air temperature and corrected wall temperature is noted in degrees Kelvin. Corrections made are to compensate for the intervening atmosphere. Infrared warming is shown by shading. Data were available in the center of the canyon for Figs. 6 (top), 7 (top), and 8 (top).

Data from the morning flights show that the north walls are warming faster than the south walls and the upper part of the walls heats faster than the lower wall. In all cases the semidesert floor is warmer than the walls even though longwave cooling occurs at night. At night, when the air in contact with the sloping ground cools, its density increases. This results in a negative buoyancy of the chilled air and stable layers within the canyon. Traces of the negative buoyancy still appear at 0930 MST in the cross section of Fig. 6 (top). This cross section represents the westerly portion of the research area (Fig. 3). Infrared warming has already replaced infrared nighttime cooling. As the day proceeds, if the sky remains clear or nearly clear, the warming layers increase in depth and turbulent mixing should exceed the top of the canyon. The ambient temperature differential from the walls, which has reached −12.7 K in the morning, will change to positive values. The degree to which this may occur is a function of sky cover and cloud thickness.

Figures 7 and 8 show the contrast of clear to broken sky cover effect on stability and heating of the canyon in October. The extreme stability of the morning canyon is shown in Fig. 7. Acceleration values even above the canyon reach as low as −0.17 m s^{-2} due to a very clear night and the fact that these data were obtained a month later than those of Fig. 6. The wall temperature

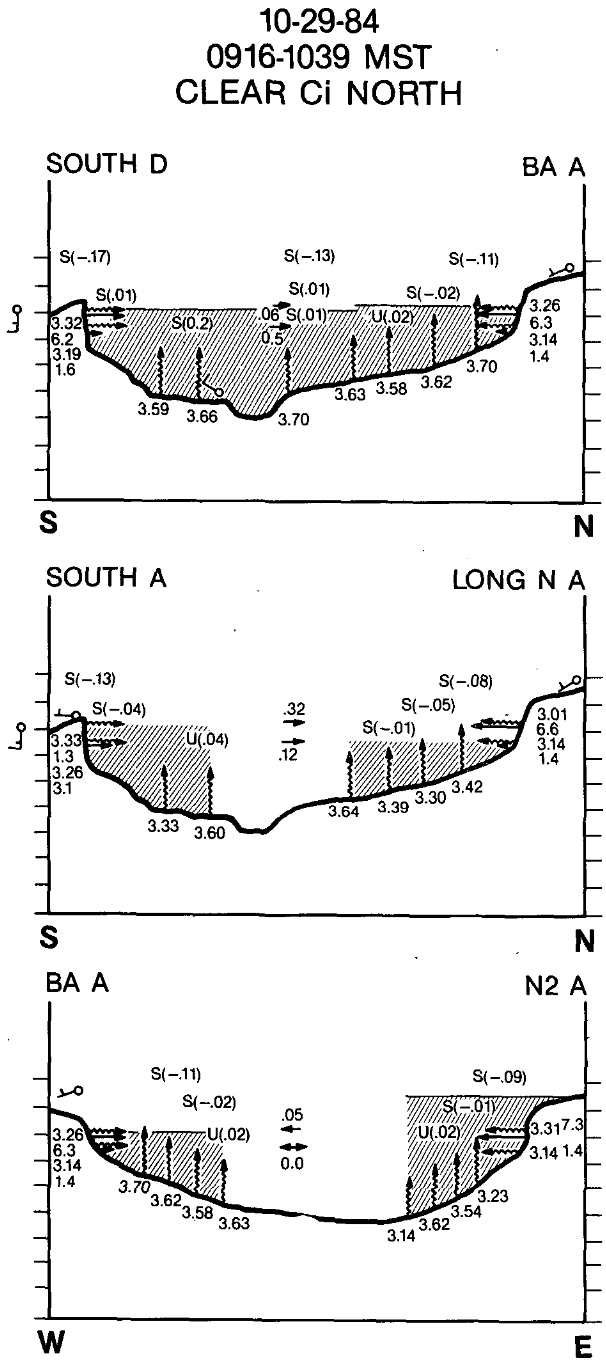

FIG. 7. As in Fig. 6, but for 29 October morning. Sunrise was at 0647 MST (1347 UTC) and sunset at 1736 MST (0036 UTC).

is warmer than the air in all cases, and infrared layer warming in addition to solar warming is occurring to a great height, especially along the south wall. However, under broken skies in the afternoon, the pattern of solar warming is interrupted (Fig. 8) and the expected destruction of the stable layer above the canyon does not occur. Furthermore, the mechanical mixing above the canyon cannot take place because of reduced solar and convective heating. Instability does occur over the canyon in some areas, but the layer at the top of the canyon remains stable.

5. Conclusions

The September data show that convective and radiational heating of the canyon are sufficient to allow mixing within the canyon to be deep enough to disrupt

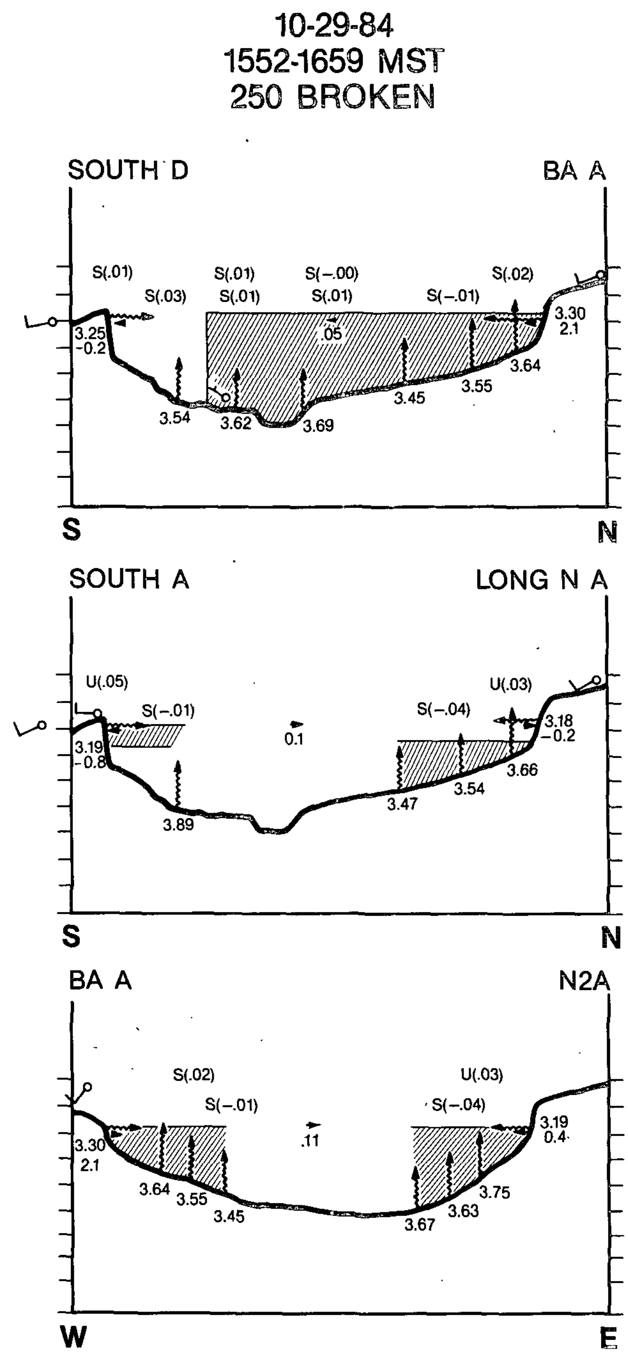

FIG. 8. As in Fig. 6, but for 29 October in the afternoon.

the morning stability capping the canyon. From aircraft missions within and above the canyon's east and south rims, a flow toward the canyon has been noted above the east rim at 2195 m (Sinclair, personal communication, 1986). Also, in some areas of the canyon, the increased temperature of the walls, due to solar heating, produces an upward motion along the walls, which flows out onto the rims. However, according to Sinclair, this air motion, although strong, especially before and at sunset, is shallow and does not extend far from the rims. The longwave radiational cooling at night is sufficient under clear skies to encourage drainage flow downstream if the synoptic flow does not interfere. The synoptic flow can enhance the canyon flow if it is roughly parallel to the canyon walls as in the case of 29 September where the easterly synoptic winds encouraged a northeasterly flow on the Tonto Plateau. A cross-canyon flow, however, has less influence on the canyon circulation, which is mostly thermally driven. Since the North Rim is higher than the South Rim by about 365 m, most of the synoptic flow is directed downward toward the center of the canyon and ahead of the thermal influence of the north wall. The remainder of the stream continues across the North Rim, modified only by local influences. If coupling is total in the situation of a cross-canyon synoptic flow, a flow nearly opposite to that above the canyon should be found. On 29 October, the Tonto Station recorded a northerly component which opposes the southerly component of the synoptic flow, but contained a heavy westerly component which was parallel to the walls and thus influenced more by wall orientation.

The following conclusions have been made on the basis of all the observations and data acquired during the fall season of 1984:

- The wind pattern within the canyon is almost parallel to the walls.
- Layered stability established at night usually reaches depths well above the canyon.
- The thermal heating pattern is well established 1.0 to 1.5 h after sunrise.
- There are none of the 19 segments of the canyon that do not receive any solar radiation due to the complex orientation of each segment.
- The disruption of the stable layers is spatially and temporally variable and is a function of the total sky cover and the cloud thickness.
- In cloudy conditions a stable layer often remains at the top of the canyon even though unstable layers may exist above it.
- The air motion within the canyon is influenced by subtle elements of the large-scale meteorological structure such as flow parallel to some segments of the canyon.
- In September, synopotic patterns have a lesser effect on the local wind regime than in late October since thermal patterns are stronger in September.
- The canyon winds are almost always upstream relative to the river flow.
- At night, longwave radiative cooling encourages stable stratification within the canyon. Warm air entrainment from above the canyon may also encourage stable stratification. Pollutants transported into the canyon by convergence or subsidence will be trapped.
- Ambient meteorological conditions can affect the canyon wind nighttime regime by hindering the basic driving force, namely radiative cooling. Strong ambient winds can retard radiative cooling by distributing the cooled air through a deeper area, reducing the temperature deficit, or by adding moisture or even clouds.

As a result of the above phenomena, the canyon was more able to cleanse itself in September than October.

Acknowledgments. The author thanks William D. Neff for encouragement and support for this work, Jorge A. Puig for his help in computer analyses, and Marilyn Van Asche and Sandra J. Furney for word processing the manuscript. The author also wishes to thank the National Park Service personnel, especially John Ray at the Grand Canyon, for courtesies extended at the park, and Donald Henderson, who was responsible for advice and arrangements necessary for the execution of this project. This research was supported by the Department of the Interior, National Park Service Interagency Agreement 0492–0082–03.

REFERENCES

Bader, D. C., and T. B. Mc Kee, 1985: Effects of shear, stability and valley characteristics on the destruction of valley inversions. *J. Climate Appl. Meteor.*, **24**, 822–832.

Banta, R., and W. R. Cotton, 1981: An analysis of the structure of local wind systems in a broad mountain basin. *J. Appl. Meteor.*, **20**, 1255–1266.

Dickerson, M. H., and P. H. Gudiksen, 1983: Atmospheric studies in complex terrain: Technical progress report FY-1979 through FY-1983. UCID-19851, Lawrence Livermore National Laboratory, Livermore, CA, 367 pp.

Post, M. J., and W. D. Neff, 1986: Doppler lidar measurements of winds in a narrow mountain valley. *Bull. Amer. Meteor. Soc.*, **67**, 274–281.

Whiteman, C. D., 1982: Breakup of temperature inversions in deep mountain valleys: Part I. Observations. *J. Appl. Meteor.*, **21**, 270–289.